Journal of Thermal Analysis and Calorimetry, Vol. 85 (2006) 1, 179–187

THE CONTRIBUTIONS OF MDSC* TO THE UNDERSTANDING OF THE THERMODYNAMICS OF POLYMERS**,***

B. Wunderlich[1,2]****

[1]Department of Chemistry, The University of Tennessee, Knoxville, TN 37996-1600, USA
[2]Chemical Sciences Division, Oak Ridge National Lab., Oak Ridge, TN 37831-6197, USA

Contributions of modern, temperature-modulated calorimetry are qualitatively and quantitatively discussed. The limitations are summarized, and it is shown that their understanding leads to new advances in instrumentation and measurement. The new thermal analysis experiments allow to separate reversing from irreversible processes. This opens the irreversible states and transitions to a description in terms of equilibrium and irreversible thermodynamics. Amorphous systems can be treated from macroscopic to nanometer sizes with weak to strong coupling between neighboring phases. Semicrystalline, macromolecular systems are understood on the basis of modulated calorimetry as globally metastable, micro-to-nanophase-separated systems with locally reversible transitions.

Keywords: *coupling between phases, irreversible thermodynamics, nanophase, reversibility, TMDSC*

Introduction

Most processes on earth are irreversible. When commercial temperature-modulated differential scanning calorimetry, TMDSC, became available [1], the level of reversibility could be studied. The TMDSC can separate irreversible from reversible effects, and many macromolecules have been analyzed in this fashion [2]. In TMDSC the response to modulation is separated from the total heat-flow rate,$<\Phi(t)>$, the sliding average of $\Phi(t)$ over one modulation period. The $<\Phi(t)>$ arises from the underlying heating rate, $<q>$ (Figs 1 and 2). The value of $<\Phi(t)>$ is not always similar to the standard DSC response (Fig. 4). The reversing heat-flow rate, $\Phi(t) - <\Phi(t)>$, is a pseudo-isothermal response to the modulation alone. The term reversing was introduced [3] together with the MDSC™ instrumentation to distinguish it from true thermodynamic reversibility. The reversing heat-flow rate is not truly reversible when its response to modulation is nonlinear, or the sliding average, $<\Phi(t)>$, is nonstationary [4].

Outside the transition ranges, total and reversing heat-flow rates are identical, an indication of reversibility of the molecular motion. In macromolecules, molecular motion consists mainly of small-amplitude vibrations and large-amplitude conformational motion. Lowering the temperature to the glass transition, the large-amplitude motion becomes cooperative and is sufficiently slow that the heat capacity becomes frequency-dependent (Fig. 7). At lower temperature, only vibrational motion is left. The kinetics of the glass transition, naturally, can be measured with TMDSC. A detailed study of the frequency dependence in the glass transition has been made on the examples of amorphous polystyrene and semicrystalline poly(ethylene terephthalate) [5, 6].

Within transition ranges which are coupled to latent heats (first-order transitions), the pseudo-isothermal deconvolution of TMDSC is frequently qualitative because of the instrument lag and a loss of stationarity due to the overwhelming amount of latent heat, and due to slow response of the sample during melting, crystallization, annealing, crystal perfection, or recrystallization (Fig. 4). To avoid this problem, TMDSC without an underlying heating rate, $<q> = 0$, a so-called quasi-isothermal analysis, was developed. In this case, modulation is forced about a constant temperature, T_o, and can be carried out for extended periods of time to await the decay of all irreversible processes occurring at T_o and the metastable state is

* MDSC, trademark for the modulated DSC of TA Instruments, Inc., introduced in 1992
** Presented in the Symposium "Modulated Techniques/Fast Scan Thermal Analysis"
*** The submitted manuscript has been authored by a contractor of the U.S. Government under the contract No. DOE-AC05-00OR22725. Accordingly, the U.S. Government retains a non-exclusive, royalty-free license to publish or reproduce the published form of this contribution, or allow others to do so, for U.S. Government purposes.
**** Wunderlich@CharterTN.net

1388–6150/$20.00

Akadémiai Kiadó, Budapest, Hungary
Springer, Dordrecht, The Netherlands

reached. The analysis is then continued at a sequence of higher or lower values of T_o.

Five different types of reversing and reversible latent heats could be established from TMDSC of a number of macromolecules [2]: Type 1 is fully reversible melting and crystallization in the presence of crystal nuclei. It is seen in paraffins, limited to chain-lengths of ≈75 atoms in the backbone (Fig. 17). In addition, sufficiently short, decoupled segments of the main-or side-chain of the macromolecule may similarly crystallize, and then behave reversibly.

Type 2 is the reversing melting which involves distributions of oligomers as they are present in low-molar-mass polymers and also in copolymers. Here, the melting peak is broadened considerably and the reversibility of melting is limited due to decoupling of the transition from changes in concentration which needs longer time to be completed. These changes in concentration are dictated by the phase diagram of a multi-component, multi-phase system when changing temperature. For poly(oxyethylene), a time-dependent change of the reversing melting was observed. The reversing, apparent heat capacity increased, as diffusion established a fluctuating concentration between the two phases (Fig. 18).

As the molar mass of a distribution of oligomers increases beyond a critical chain-length of ≈75 atoms, the melting usually does not become fully irreversible, but a small amount of Type 3 reversing melting remains for the extended-chain crystals. The Type 3 reversing melting decreases with increasing chain length and crystal perfection, as first documented for extended-chain crystals of polyethylene [7]. The fusion of extended-chain crystals, thus, is largely irreversible (Fig. 19).

Type 4 reversing melting is seen in folded-chain crystals and a portion of it may represent a local melting equilibrium at their surface as seen in Figs 19–21. The reversing latent heat decreases with time before reaching residual reversibility. The decrease in latent heat involves changes in melting, crystallization, annealing, crystal perfection, or recrystallization [2].

From paraffins to polyethylene, one always observes an additional, Type 5 of excess reversible heat capacity which is linked to local gauche-trans-equilibria. These local equilibria exist in the crystal and glass of polyethylene, starting far below the transition temperatures. They are better considered as part of the heat capacity, but in the past, have often been discussed as transition phenomena, hence the name: Type 5. For polyethylene, Type 5 is of special importance in the thickening of folded-chain crystals through sliding diffusion. As shown in Fig. 22, an even bigger effect is observed in poly(oxyethylene). It has been suggested that this effect can be interpreted as the glass transition of the crystals [8]. The crystals of macromolecules affect also the glass transition of the surrounding amorphous phase and may produce a rigid-amorphous nanophase. Its properties can similarly be studied by TMDSC [2].

After this introductory summary, details will be discussed. In most cases a bare beginning has been made. Especially, glass transitions are often overlooked in the investigation of multi-phase systems.

Experimental

A typical differential scanning calorimeter, DSC, is illustrated in Fig. 1, and the responses when using it in the DTA, DSC, or TMDSC mode are shown in Fig. 2. The equations in Fig. 1 reveal that it is a simple matter of calibration and correction to report the thermodynamic quantity specific heat capacity of the sample, c_p, in J K^{-1} mol^{-1} (instead of the heat-flow-rate data, $\Phi(t)$, which are equal to $K\Delta T$, or KA_Δ). The other quantities in the equations of Fig. 1 are m, the sample mass, q, the heating rate, C_s, the heat capacity of the sample and pan, C_r the heat capacity of the reference pan, A, the particular modulation amplitude, ω, the frequency in 2π/(modulation period in seconds), and K and τ are constants. These constants are usually fitted by calibration, although K is Newton's constant of heat conduction, and τ approaches at low frequency the value $C_r\omega/K$, as shown in Fig. 3.

From Fig. 2, it can be seen that DTA and DSC data reach steady state after about 100 s. As soon as this steady state is reached, quantitative evaluations of the data can be made using the left equation of Fig. 1. For TMDSC, steady state may never be reached at modulation periods of less than 100 s, but the analysis is still possible as long as the response is linear, i.e., the changes in T_s and fraction of trans-

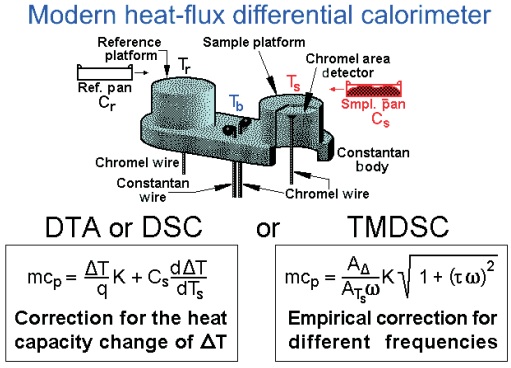

Fig. 1 DTA, DSC or TMDSC. Note that K and τ are constants, and for TMDSC, $q(t) = A_{T_s}\omega$. The second terms in both equations are corrections for changes of the specific heat capacity, c_p, with temperature and frequency, respectively

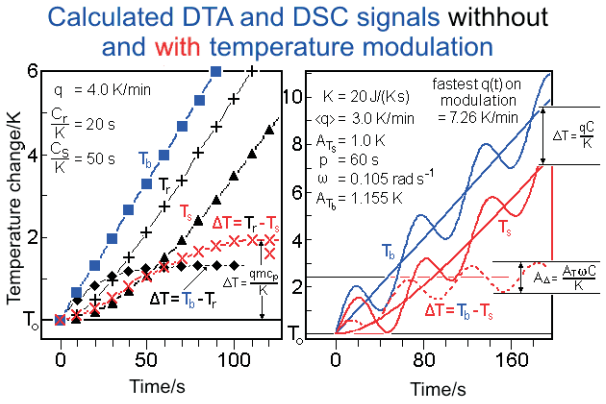

Fig. 2 Response of DTA, DSC and TMDSC to changes in the block temperature, T_b. Note that for clarity the temperature difference (response) on the left (DTA or DSC) is $T_r - T_s$, while on the right (TMDSC) it is $T_b - T_s$, resulting in a different C

formed material yielding a latent heat is proportional to ΔT at the given instant.

Figure 3 illustrates the calibration of TMDSC with quasi-isothermal sawtooth modulation [9]. The experimental heat-flow rate is represented by its harmonics. Each harmonic is treated as given in Fig. 1. The insert at the bottom left shows the constancy of the slope, τ, for low frequencies, and the right Fig. 3 illustrates the precision, which can reach ±0.1%. The crystals and the melt of In in Fig. 4 illustrate the same response as long as no melting or crystallization occurs. The calibration was done at frequency $2\pi/p$.

In Fig. 4 after approximately 97 min, melting of some In is observed. Before completion, melting is reversed by quick recrystallization. As the underlying heating rate increases the maximum temperature,

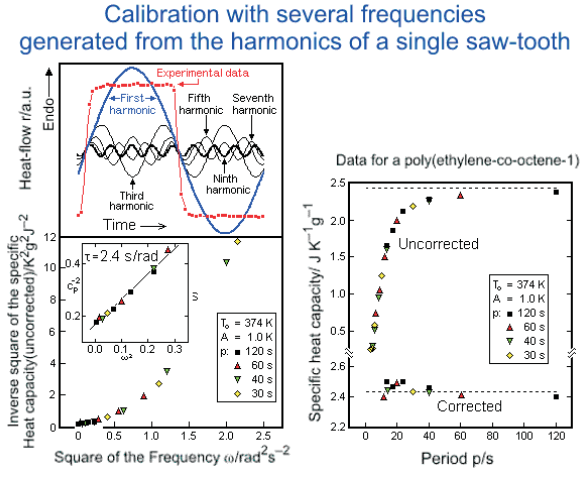

Fig. 3 Upper left: Experimental heat-flow rate and the first nine harmonics of the TMDSC heat-flow-rate response to the temperature modulation. Bottom left: Evaluation of τ. Bottom right: Evaluation of c_p according to Fig. 1 (right equation)

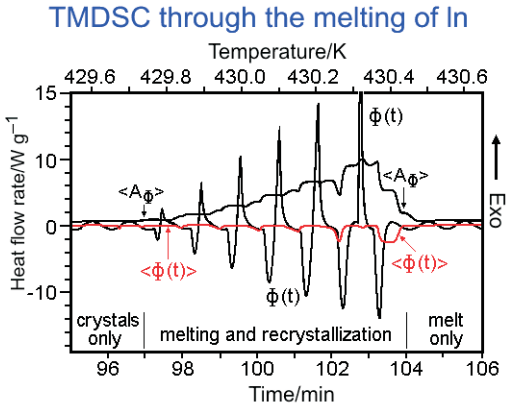

Fig. 4 Heat-flow-rate data, $\Phi(t)$, proportional to ΔT; total heat-flow-rate, $<\Phi(t)>$, which should be similar to the standard DSC (but is not, due to nonstationarity); and the deconvoluted, averaged, reversing amplitude $<A_\Phi> = <\Phi(t) - <\Phi(t)> >$

more and more In can melt, until finally all is melted at 104 min. The slope of the connection between melting and crystallization peak indicates the calorimeter response, and before the last crystallization peak, the need of nucleation. The analysis of the experimental heat-flow rate $\Phi(t)$ reveals the nonstationary character of the result. The sliding average, the total heat-flow rate $<\Phi(t)>$ is not equal to a standard DSC trace which shows only a single, sharp melting peak. The calculated (once more averaged) amplitude of the reversing heat-flow rate has, as one would expect, contributions, both, from melting and crystallization as a positive response. This larger amplitude leads to a larger apparent c_p and latent heat, but its quantitative features are limited because of the erroneous deconvolution of the data.

Amorphous polymers

The glass transition temperature, T_g, of an amorphous material marks the separation between solid and liquid. In the solid state, practically the only molecular motion is fast, small-amplitude vibration (10^{-12}–10^{-14} s), in the liquid state, some of these vibrations change to much slower, large-amplitude motion. In macromolecules, the large-amplitude motion is almost exclusively conformational motion (0–10^{-12}s). Figure 5 depicts the change of the heat capacity from that of the glass to the liquid and its five characteristic temperatures, T_g, T_1, T_2, T_b, and T_e, the change in heat capacity, ΔC_p, and the cooling rate, q. The glass transition is characterized by slow, cooperative processes which are amenable to study with TMDSC.

The schematic of Fig. 6 illustrates the changes in enthalpy on cooling and heating through the glass

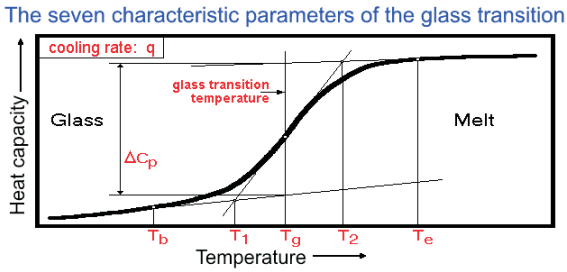

Fig. 5 Schematic of the change of the heat capacity in the glass transition region. Listed in the figure are the parameters that must be given for full characterization

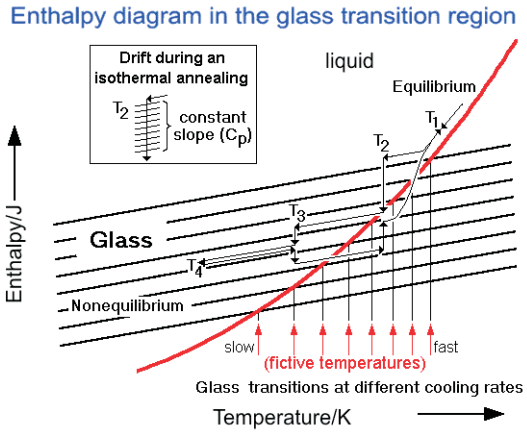

Fig. 6 Schematic of the enthalpy in the glass transition region on cooling into the glassy state. Stepwise cooling, two stages of annealing, and reheating are indicated at T_1 to T_4

transition region. The heat capacity is to be noted as the slope of the enthalpy, H. The drift toward lower or higher enthalpy on annealing is shown in the insert as a slow (irreversible) change in H, while the slope measured by the much faster modulation, is close to the same for all glasses and has a reversing character. The response to the two time scales, thus, in this case can be separated by TMDSC.

Figure 7 illustrates the change of the glass transition with frequency, as measured by quasi-isothermal TMDSC on polystyrene and extrapolated to higher frequency [5], using a simple hole model of the glass transition which applies a first order kinetics and an Arrhenius-type activation energy. The change of the hole concentration on cooling in a standard DSC experiment is shown in Fig. 8 [10]. The separate freezing of the fast modulation effect and the slow underlying cooling is clearly visible.

Figure 9 makes use of the same computation scheme to calculate the total, reversing, and non-reversing heat capacity. Besides separation of the two components of the total C_p, one notices remaining modulation. This is an indication of the change in frequency when superimposing two time scales [11].

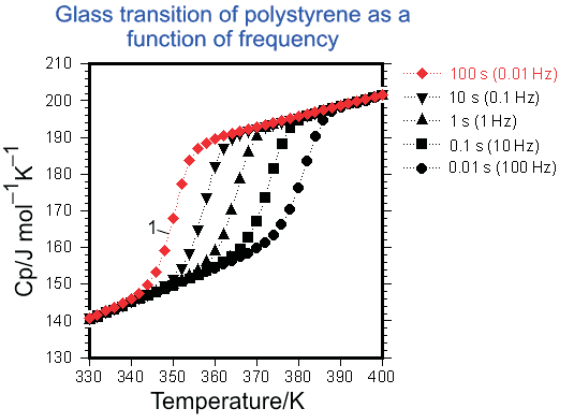

Fig. 7 Change of the glass transition of polystyrene as a function of modulation frequency. The measured, quasi-isothermal data range from 0.01 to 0.033 Hz (1). The additional values are extrapolated using a simple hole model [5]

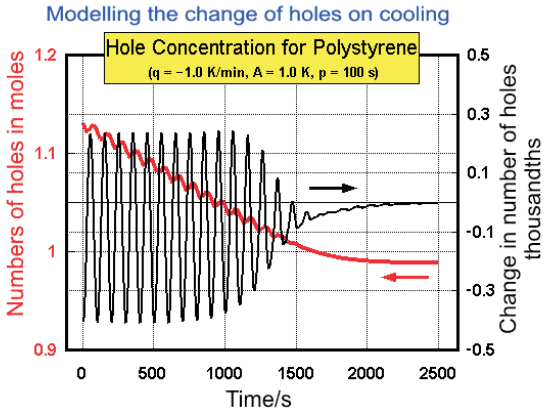

Fig. 8 Change of the number of holes during TMDSC with an underlying cooling rate, to show the separation of the two time scales of freezing of large-amplitude motion. The heat capacity on reheating of the cooled sample is shown in Fig. 9

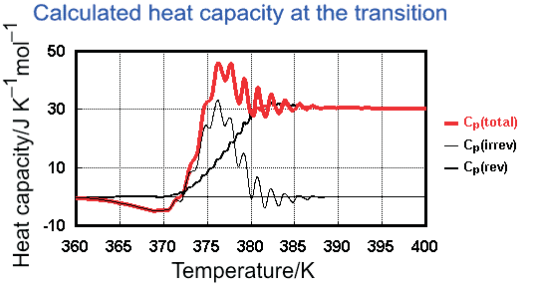

Fig. 9 Heat capacity contributions in the glass transition region, calculated from quasi-isothermal experiments as illustrated in Fig. 8. The remaining modulation is a Doppler-like effect from the interference of the two time scales

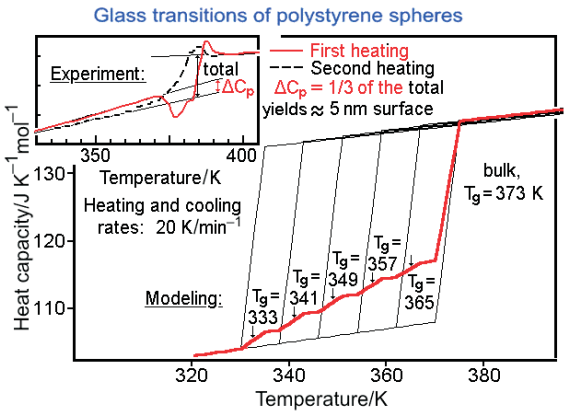

Fig. 10 Change of the glass transition of polystyrene in 85 nm diameter beads (insert). Besides the exotherm, signaling the strain-release due to coalescence, the ΔC_p is reduced by 1/3, modeled by successive layers from outside to inside [10]

A different influence on the glass transition is seen when reducing the phase-size of the polymer, as was analyzed for polystyrene spheres and block copolymers [12]. In this case one can observe a decrease in T_g on the surface of the spheres, as illustrated in Fig. 10, while in the block copolymers the glass transition may increase in case of restraints at the interface, and decrease when the interface is more mobile. This result is of importance when studying more complicated multi-phase semicrystalline polymers, where with TMDSC the behavior of the phases can be separately investigated.

Semicrystalline polymers

The typical phase-structure of macromolecules is known for quite some time. Figure 11 illustrates an early suggestion for a high-crystallinity polymer fiber. The two assumed phases are metastable micro- to nanophase crystals and an amorphous phase which may be far from the state of the fully amorphous glass or liquid, and also be of nanophase dimension. Figure 12 illustrates the typical semicrystalline behavior of poly(butylene terephthalate). Only by deconvolution of the reversing apparent heat capacity from the total, is it possible to properly identify the cold crystallization above 300 K and see that the crystallization continues to increase up to the melting region (see insert). For the analysis of the crystallinity, it is necessary to identify the rigid-amorphous fraction, RAF, and also find its separate glass transition at about 400 K to insert the proper, temperature-dependent heat capacities into the equation of Fig. 12.

The glass transition of an amorphous and semicrystalline PET is shown in Fig. 13 [6]. There are two effects seen, first, the glass transition is broadened in

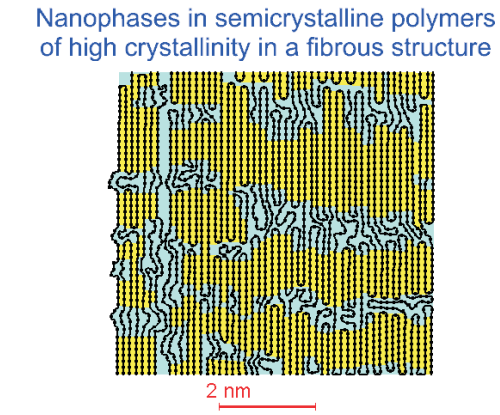

Fig. 11 Schematic of the structure of the globally metastable, semicrystalline fibers as suggested some 40 years ago by Hosemann, based on mainly X-raydiffraction

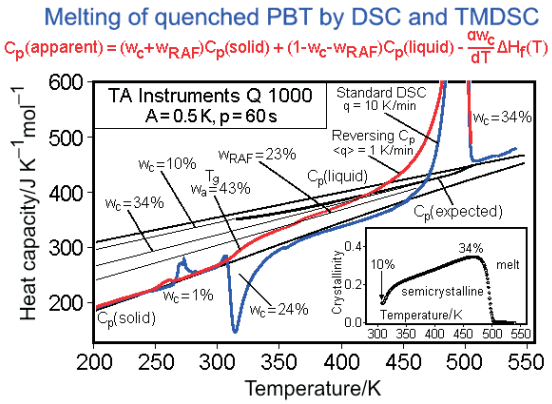

Fig. 12 Standard DSC and TMDSC of poly(butylene terephthalate). The insert shows the change in crystallinity on heating as calculated with the above equation

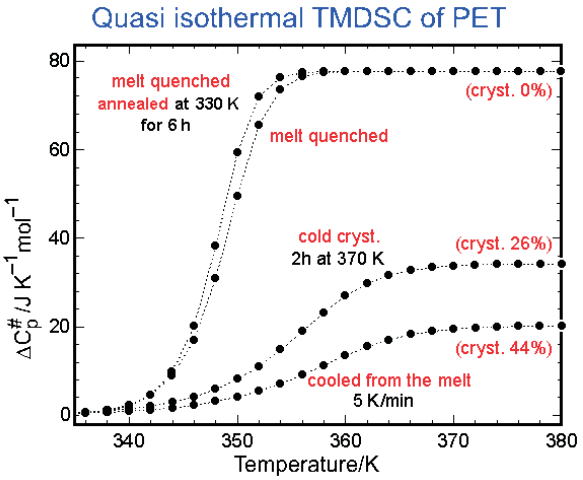

Fig. 13 Change of the apparent reversible heat capacity of poly(ethylene terephthalate) in the glass transition region as measured by quasi-isothermal TMDSC. Two effects are seen, a broadening on partial crystallization and a change in ΔC_p

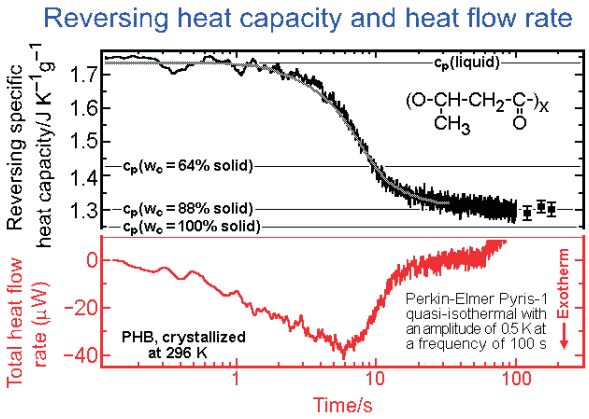

Fig. 14 Total heat-flow rate, proportional to the latent heat of crystallization, and the reversing, specific capacity from quasi-isothermal TMDSC of poly(3-hydroxybutyrate), PHB, at 296 K during crystallization [12]

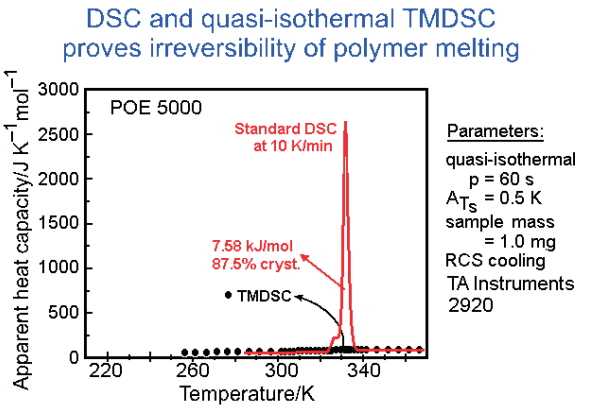

Fig. 16 Standard DSC and TMDSC of the melting of extended-chain crystals of a 4540 Da (POE5000). The sample melts practically fully irreversible, the remaining Type 3 reversing melting is barely detectable [15]

crystallization, and second, the magnitude decreases by a larger amount than expected from the crystallinity available from the heat of fusion. The broadening reveals a changed kinetics which could be quantified from the data in Fig. 13 [6]. The discrepancy in ΔC_p is made up by the rigid-amorphous fraction. Its separate, higher glass transition reveals that it must be a separate phase. One assumes it to be a nanophase since it has no bulk material within its glass transition region. Turning to the isothermal crystallization data in Fig. 14, one can see that the decrease in heat capacity does not stop at the value expected for the ultimately reached crystallinity of 64%, but drops further to an 88% solid sample, i.e., indicating an RAF of 24%. The exothermic heat of crystallization can be read from the total heat-flow rate of the lower graph of Fig. 14. Taking both curves together one can make it likely that the crystal and the RAF form quantitatively at the same instant [13].

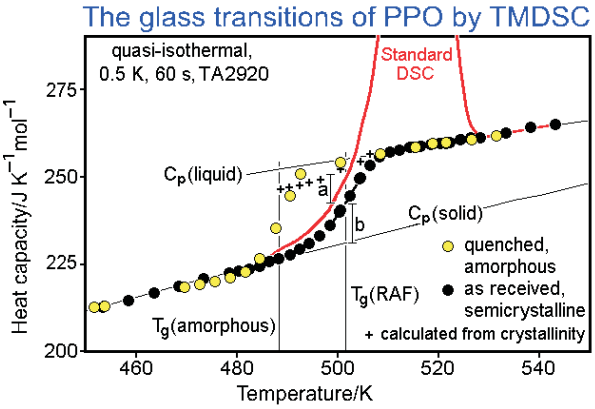

Fig. 15 Apparent heat capacity of poly[oxy-1,4-(2,6-dimethylphenylene)], PPO, measured by standard DSC and quasi-isothermal TMDSC. The crystallinity of the semicrystalline PPO is ≈30% [14]

A special case of RAF arises in Fig. 15 [14]. The 30% crystalline sample shows no glass transition, i.e., all 70% noncrystalline PPO are RAF. In addition, melting becomes only possible after the glass transition. The RAF, indicated by the length 'a' in the figure decreases parallel with the melting of the sample, but all crystals can be melted at about 500 K. One notices also, that the glassy phase surrounding the crystal eliminates all reversing melting of semicrystalline PPO indicated by the filled circles.

Figure 16 displays an example of melting of an extended-chain crystals the of poly(oxyethylene) of low molar mass [15]. All heat of fusion is absorbed irreversibly. Decreasing the chain-length of such crystals below ≈75 chain atoms, this melting is practically all reversible, as illustrated in Fig. 17 on the example of the *n*-paraffin $C_{50}H_{102}$ [16]. Such melting was listed in the Introduction as Type 1 reversible melting. Figure 18 is an example of Type 2 reversing melting

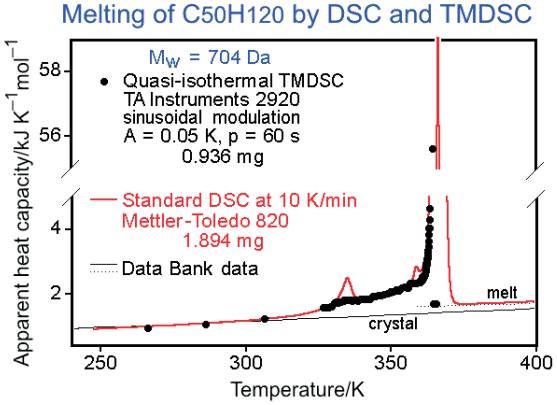

Fig. 17 Standard DSC and quasi-isothermal TMDSC of pentacontane, $C_{50}H_{102}$, a pure paraffin. The melting is practically fully Type 1 reversible melting. The two small irreversible DSC peaks are probably due to impurities. The standard DSC trace is broadened due to instrument-lag

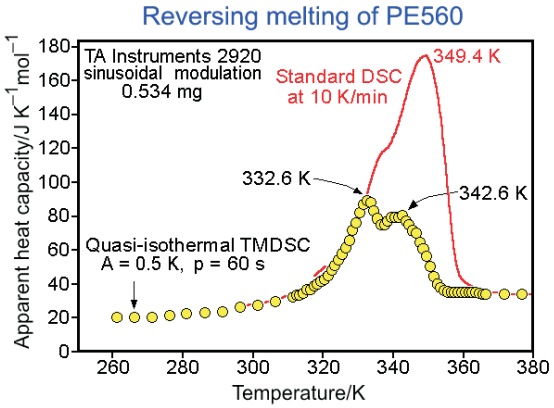

Fig. 18 Standard DSC and quasi-isothermal TMDSC of a fraction of polyethylene oligomers of an average chain-length of 44 chain atoms (PE560). The eutectic system shows first full reversibility, then, the response becomes only partially reversible, because of slow diffusion to and from the crystals

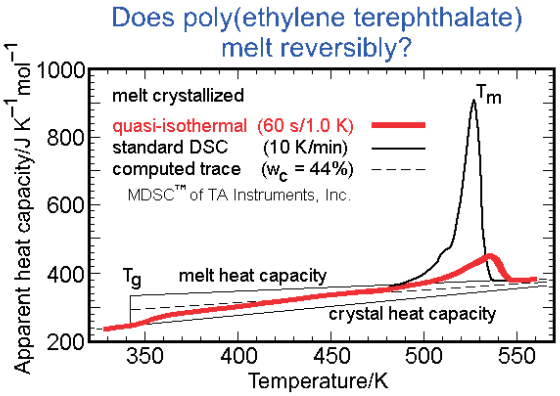

Fig. 20 Standard DSC and quasi-isothermal TMDSC of melt-crystallized PET. The two-step glass transition and annealing during TMDSC is visible. As described in the text, the reversing contribution to the apparent C_p is of Type 4 [18]

[17]. The reversibility exists only on the low-temperature side of the melting peak. At the higher temperatures within the broad melting peak, caused by the eutectic phase diagram of the multi-component system, the system cannot follow the modulation since it requires major readjustment in the concentration throughout the melt, so that the melting and crystallization increasingly decouple from the mixing and demixing in the melt.

Figure 19 illustrates the change in reversing melting of largely extended-chain crystals of polyethylene fractions (with the average molar masses given in daltons expressed by the sample number) from the Type 1 and 2, seen in PE560 of Fig. 18, to mainly Type 2 and 3 in the fractions PE1150 and 2150, to finally a combination of all three types for the broad-molar-mass, extended-chain crystals of PE130000. The PE130000 analysis was fully quantitative [7] and led to a mainly irreversibly melting polymer. This analysis and the results in Fig. 16 suggest that perfect extended-chain crystals are equilibrium crystals, but do not melt reversibly since their crystallization is hindered by crystal and molecular nucleation [4].

A large surprise was seen when analyzing the TMDSC data in Fig. 20 [18]. When waiting long times, as shown in Fig. 21, the initially reversing melting and recrystallization, indeed, becomes reversible. This is the Type 4 reversing and reversible melting which has by now been documented for many polymers and copolymers [2]. A complication of the quantitative analysis of Type 4 melting was seen in an uncertainty of the baseline, the Type 5 melting effect. The poly(oxyethylene) melting in Fig. 22 shows that

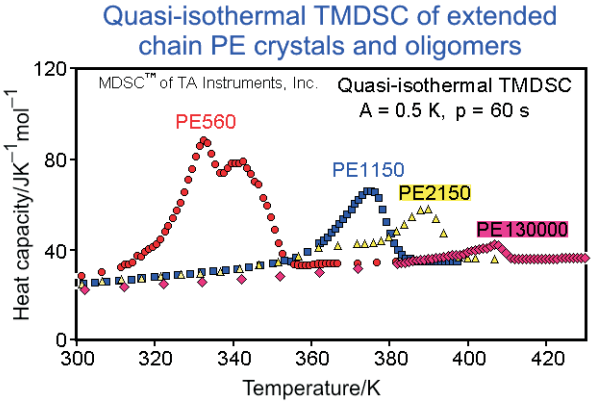

Fig. 19 Quasi-isothermal TMDSC of a series of extended chain crystals of polyethylene fractions and a broad-distribution polymer, PE130000. The number indicates the mass-average molar mass. Data with Type 1, 2 and 3 reversing melting

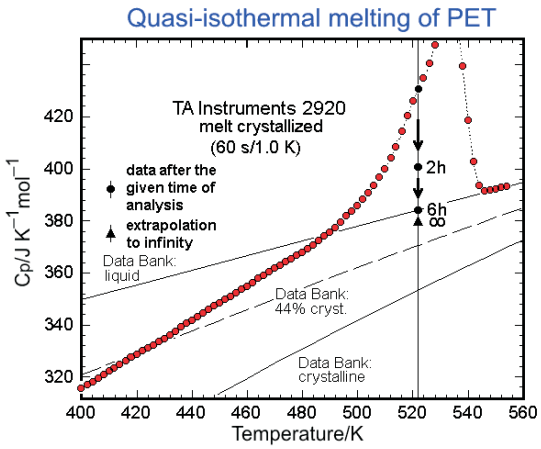

Fig. 21 Enlarged plot of the quasi-isothermal TMDSC of PET from Fig. 20. The black circles indicate experiments, used for the long-time experiment. Extrapolation of the data to infinity, using two relaxation times, yields the point at ∞ , where the Type 4 melting becomes reversible

this uncertainty is due to conformational motion which leads to a C_p of the crystals that reaches the value of the melt and make Type 5 melting a true, thermodynamic heat-capacity effect [8].

Conclusions

The 22 figures, chosen mainly from work in our own laboratory, document the advance temperature-modulated calorimetry has brought to thermal analysis of amorphous and crystalline polymers. The experimental hurdles can be overcome, as shown in Figs 1–4. The more exacting needs of TMDSC have also led to improvement of the available calorimetric instrumentation. As the present symposium indicates, the renewed interest in time as a parameter of calorimetry has also catalyzed the advances in fast calorimetry, which by its nature has to work with very small samples [19]. Quantitative data at time scales of microseconds, unthinkable only 10 years ago, are now possible and will be needed to unlock the calorimetry contained in nanophase structures as suggested in Fig. 11 [20].

It became obvious early in its application that, even more than qualitative DSC, qualitative TMDSC is only of limited value. It is vital to concentrate on the development of quantitative thermal analysis. Quantitative DSC permitted the extraction of the basic equilibrium thermodynamics from nonequilibrium data by appropriate extrapolation and modeling based on molecular motion. Quantitative TMDSC has helped to delineate equilibrium from irreversible thermodynamics. This is a process which takes much more time than the development of the link from macroscopic morphology to atomic structure, and also takes many more scientists who will take-on the challenge to produce quantitative data and the connection to molecular motion that underlies the thermal properties. The main reason for the greater difficulty to achieve an understanding of molecular motion relative to structure lies in the larger distance of the former from the human scale of perception [4]. Molecular structure with its basic unit, the ångstrom, is by a factor 1/10.000 smaller than the tiniest visible thing of micrometer-size (10^{-6} m, visible with an optical microscope). Molecular motion, in contrast, with its basic unit, the picosecond (10^{-12} s), is by a factor 1/1.000.000.000 faster than the quickest event that can be followed by eye (needing perhaps a millisecond, 10^{-3} s).

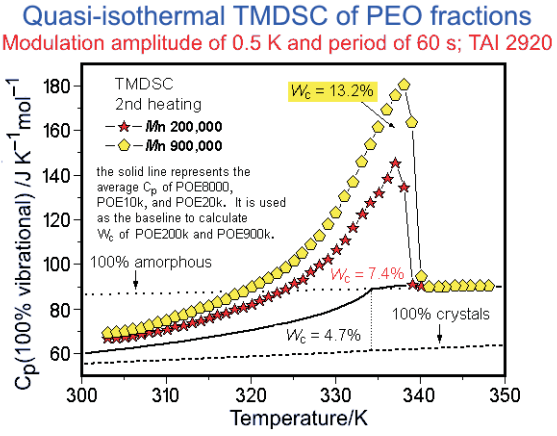

Fig. 22 Quasi-isothermal TMDSC of two high molar-mass poly(oxyethylene)s. The solid baseline indicates the increase in thermodynamic heat capacity due to conformational motion (Type 5 reversible melting). When integrated over *T*, this contribution yields an equivalent error of 4.7% crystallinity

The amorphous polymers are characterized thermodynamically, besides their heat capacity, by the glass transition, as shown in Fig. 5, which separates the solid from the liquid state. Glass transitions are basically irreversible, as illustrated in Figs 6–9. The main problem of the description is the cooperativity of the glass transition. Figure 6 illustrates that there are many glassy states with different free enthalpies, and it was shown that even the same free enthalpy may belong to more than one glass. The simple descriptions offered in Figs 8 and 9 illustrate glass-like behavior, but actual glasses need an adjustment of the simple kinetic parameters [21]. The unsophisticated description of Figs 6–9 reveals that measurement with an underlying heating rate leads to an interference between the two time scales, changing the frequency of the response from that of the sample temperature, i.e., the first harmonic used for the analysis needs to be corrected with at least a second harmonic and a frequency shift [11]. The size-and strain-dependence across phase areas from continuing molecules are two additional topics of great importance [12]. They can now be tackled quantitatively by extending the standard DSC analysis as in Fig. 10 to TMDSC.

The crystalline polymers offer an even more interesting field of research as illustrated in Figs 11–22. The phase-structure in Fig. 11 is still too simple for the description of semicrystalline polymers. The rigid-amorphous nanophase is shown to be important for many systems, as shown in Figs 12–15. The irreversible melting of semicrystalline polymers has been verified, but only for crystals surrounded by glassy portions of molecules (Fig. 15), extended-chain crystals (Fig. 16), and precisely folded lamellae [8]. The five Types of reversing melting, summarized in the Introduction, have been substantiated in Figs 17–21. Figure 22, finally, documents that on crystallization, the ordering and freezing of conformational motion

do not have to occur simultaneously. A crystal can have a glass transition without being a mesophase!

Only a small list of applications of TMDSC was covered in this lecture. Other materials, such as mesophases, copolymers, fibers and films, and small molecules can be studied by TMDSC. Chemical thermodynamics also is gaining from modulated calorimetry, as was shown by the simultaneous study of irreversible chemical reactions during curing and the reversible changes in heat capacity [4]. Furthermore, TMDSC for defect identification in polymers [22] and for study of hard-material physics has hardly begun.

Acknowledgements

The ATHAS effort is supported by the Polymers Program of the Materials Division of the National Science Foundation and the Division of Materials Sciences and Engineering, Office of Basic Energy Sciences, U.S. Department of Energy at Oak Ridge National Laboratory, managed and operated by UT-Battelle, LLC, for the U.S. Department of Energy, under contract number DOE-AC05-00OR22725.

References

1 M. Reading, B. K. Hahn and B.S. Crowe, 1993, U.S. Patent, Method and Apparatus for Modulated Differential Analysis, 5,224,775, July 6.
2 B. Wunderlich, Progress Polym. Sci., 28 (2003) 383.
3 M. Reading, D. Elliott and V. Hill, Some Aspects of the Theory and Practice of Modulated Differential Scanning Calorimetry. Proc. 21st NATAS Conf. in Atlanta GA, Sept. 13–16, 21 (1992) 145.
4 B. Wunderlich, Thermal Analysis of Polymeric Materials, Springer, Berlin 2005.
5 A. Boller, I. Okazaki and B. Wunderlich, Thermochim. Acta, 284 (1996) 1.
6 I. Okazaki and B. Wunderlich, J. Polym. Sci., Part B: Polym. Phys., 34 (1996) 2941.
7 J. Pak and B. Wunderlich, J. Polym Sci., Part B: Polym. Phys., 40 (2002) 2219.
8 W. Qiu, M. Pyda, E. Nowak-Pyda, A. Habenschuss and B. Wunderlich, Macromolecules, 38 (2005) 8454
9 R. Androsch and B. Wunderlich, Thermochim. Acta, 333 (1999) 27.
10 B. Wunderlich, Thermochim. Acta, 402 (2003) 1.
11 L. C. Thomas, A. Boller, I. Okazaki, and B. Wunderlich, Thermochim. Acta, 291 (1997) 85.
12 U. Gaur and B. Wunderlich, Macromolecules, 13 (1980) 1618.
13 C. Schick, A. Wurm, and A. Mohammed, Colloid Polymer Sci., 279 (2001) 800.
14 J. Pak, M. Pyda and B. Wunderlich, Macromolecules, 36 (2003) 495.
15 K. Ishikiriyama and B. Wunderlich, Macromolecules, 30 (1997) 4126.
16 J. Pak and B. Wunderlich, J. Polym. Sci., Part B: Polymer Phys., 38 (2000) 2810.
17 J. Pak and B. Wunderlich, Macromolecules, 34 (2001) 4492.
18 I. Okazaki and B. Wunderlich, Macromolecules, 30 (1987) 1758.
19 B. Wunderlich, Fast and Super-fast DTA and Calorimetry, Proc. 32nd NATAS conf. in Williamsburg, VA, Oct. 4–6, M. J. Rich, edt. CD edition, 32 (2004) 018.04.569/1–10
20 B. Wunderlich, Thermochim. Acta, 355 (2000) 43.
21 B. Wunderlich, A. Boller, I. Okazaki and S. Kreitmeier, J. Thermal Anal., 47 (1996) 1013.
22 B. G. Sumpter, D. W. Noid, G. L. Liang and B. Wunderlich, Adv. Polym. Sci., 116 (1994) 27.

DOI: 10.1007/s10973-005-7347-7